Am J Transl Res 2022;14(6):3769-3782
www.ajtr.org /ISSN:1943-8141/AJTR0142686

Original Article

Prognostic role of NLGN2 and PTGDS in medulloblastoma based on gene expression omnibus

Zhangping Ren[1*], Ming Gao[1*], Wei Jiang[2]

[1]Department of Pediatrics, Affiliated Ezhou Central Hospital, Ezhou City 436000, Hubei, PR China; [2]Department of Neurosurgery, Tongji Hospital, Tongji Medical College, Huazhong University of Science & Technology, 1095# Jiefang Avenue, Wuhan 430030, Hubei, PR China. [*]Equal contributors.

Received March 4, 2022; Accepted May 17, 2022; Epub June 15, 2022; Published June 30, 2022

Abstract: Background: Medulloblastoma (MB) is the most common intracranial malignant tumour in children, but genes and pathways involved in its pathogenesis are still under investigation. This study was designed to screen and identify biomarkers of MB to provide markers for clinical diagnosis and prognosis assessment. Methods: The data sets of GSE109401 and GSE42656 were acquired from Gene expression omnibus (GEO). Limma package in R was adopted to identify the differentially expressed genes (DEGs), and the GSE30074 data set was adopted to analyse their prognostic role. Children with MB (n=55) diagnosed in Affiliated Ezhou Central Hospital were enrolled and assigned to the patient group, and healthy children (n=30) who received physical examination in our hospital during the same time period were assigned to the control group. The two groups were compared in serum NLGN2 and PTGDS levels, and all patients were followed up for three years to understand the associations of Neuroligin 2 (NLGN2) and Prostaglandin D2 synthase (PTGDS) with the survival of patients. Results: With Limma, 247 DEGs were screened out. The LASSO-Cox regression analysis revealed that 6 genes were associated with MB prognosis, and the established model revealed a lower survival rate in the high-risk group. According to Cox regression analysis, NLGN2 and PTGDS may be independent prognostic factors of MB. Similar to the data sets, the Real time-quantitative polymerase chain reaction (RT-qPCR) assay revealed lowly-expressed NLGN2 and PTGDS levels in MB patients, and patients with lower expression of them showed a lower 3-year survival rate. Conclusion: With low expression in MB cases, NLGN2 and PTGDS have high prognostic value for MB.

Keywords: GEO, PRAMEF22, NEK2, UMPS, medulloblastoma, diagnosis, prognosis

Introduction

Medulloblastoma (MB) is identified as a Grade IV tumour by the WHO [1]. According to statistics in 2016, MB accounted for 15-20% of all tumours in children's central nervous systems [2]. According to epidemiologic data, the annual incidence of MB worldwide is 0.20-0.58/100,000 [3]. MB can involve individuals at any age, especially the individuals from 6-8 years old [4]. As a highly malignant embryonic tumour, MB is primarily located in the midline of the cerebellum, and approximately 30% of patients have metastasis at diagnosis because the tumour cells detach easiliy and circulate with cerebrospinal fluid [5]. The common treatments for MB include surgical resection, radiotherapy, and chemotherapy. However, children under 7 years old usually have a low tolerance to these drugs [6]. The selection of appropriate treatment depends on clinical subgroup, stage, resection range, location, and patients' tolerance of treatment [7].

In order to improve the treatment efficacy, MB is classified into four clinically and molecularly different subgroups based on the genetic and epigenetic methods, and it can also be divided into WNT, SHH, Group 3 and Group 4 molecularly [8]. WNT and Group 3 are the subgroup with the best and worst prognosis, respectively. Despite significant diagnostic advances, MB is still fatal for many patients, with a mortality of approximately 30% [9]. Over the past few years, an increasing number of studies have discovered that multiple genes are independent prognostic factors in MB. For instance, FAT1 gene is strongly correlated with the prognosis of MB in

Table 1. Data set information

Data set	Platform	Sample size (cancer/control)	Application
GSE109401 [13]	[HuGene-2_0-st] Affymetrix Human Gene 2.0 ST Array [transcript (gene) version]	24 (19/5)	Differentially expressed genes (DEGs) recognition
GSE42656 [14]	Illumina HumanHT-12 V3.0 expression beadchip	17 (9/8)	DEGs recognition
GSE30074 [15]	[HuGene-1_0-st] Affymetrix Human Gene 1.0 ST Array [transcript (gene) version]	30 (30/0)	Prognosis verification

children [10]. In other research, CDK4 inhibitor, a member of cyclin-dependent kinase, was found to inhibit retinoblastoma protein phosphorylation and lead to G1 phase arrest in a patient-derived MB xenotransplantation model [11]. However, few reliable biomarkers have been found to guide the clinical treatment of MB. Therefore, discovering more biomarkers is urgent to lower the MB-associated mortality and improve the prognosis of MB.

Over the past few years, bioinformatic analysis has been extensively applied in survival prediction of patients with tumor and analysis of functional pathways and genome level to improve clinical treatment efficacy. With Gene Expression Omnibus (GEO), 2 MB data sets were adopted for the analysis in present study [12]. In one GEO data set, the association of gene features with the survival of MB was established. Finally, the prognostic significance of NLGN2 and PTGDS in MB was confirmed by clinical verification.

Materials and methods

GEO data sets

We retrieved MB-associated microarrays from GEO, a public database that provides high-throughput gene expression data, chips, and microarrays. We obtained three data sets (GSE109401, GSE42656 and GSE30074) (**Table 1**). We transformed the probes into the corresponding gene symbols based on the platform annotation information.

Synthesis of matrix files and identification of DEGs

In order to merge multiple data sets, we first merged the data sets with inSilicoMerging [16], namely merging the GSE109401 and GSE42656 data sets into the matrix before_merge.tx. Then, we used the method of Johnson et al. [17] to eliminate the batch effect, and finally get the matrix after_merge.txt after elimination of the batch effect. A total of 41 samples were included in the file, including 28 cancer samples and 13 control samples. Limma package was used for screening DEGs based on a generalized linear model [18]. We adopted limma (version 3.40.6) for differential analysis to acquire DEGs between different comparison groups and control groups, with Log fold change (Log FC) threshold: 2 and False Discovery Rate (FDR) value <0.05.

Gene enrichment analysis

The analyzed DEGs were subjected to Gene Ontology (GO) and Kyoto Encyclopedia of Genes and Genomes (KEGG) pathway enrichment analysis using the "clusterProfiler" R package [19-21].

Identification of Hub genes

GSE30074 data set was treated by univariate Cox regression analysis to identify central genes associated with overall survival (OS). The Hub genes associated with the OS with P<0.05 were deemed notably significant and included in the later analyses.

Establishment of LASSO prognosis model

The pipeline of LASSO regression was adopted to filter overlapping DEGs and DMG to narrow the range of target genes. With univariate Cox analysis, survival-associated genes were screened out. The hazard risk (HR) of Cox regression model was analyzed by glmnet and survival packages [22]. The formula:

Risk scores = $\sum_{i}^{n} Xi \times Yi$. (X: coefficient of each gene, Y: expression of every gene).

Based on the median score, MB patients from GEO were assigned to low- or high-risk groups.

Table 2. Primer sequences

Gene	Upstream primer	Downstream primer
NLGN2	CTCTTGCTCGAGTGAAACCAA	CTCTGAAGGAGGGTGGATGG
PTGDS	GTGTCAGTGGTGGAGACCGA	CTGCCTGCCTCTAATCTGACCT
GAPDH	CTGGGCTACACTGAGCACC	AAGTGGTCGTTGAGGGCAATG

Note: Neuroligin 2 (NLGN2); Prostaglandin D2 synthase (PTGDS); Glyceraldehyde-3-phosphate dehydrogenase (GAPDH).

Kaplan-Meier (K-M) survival curve was adopted to analyse and compare the OS of the two groups, and time-associated Receiver operating characteristic (ROC) was drawn to evaluate the predictive value of gene markers.

Univariate and multivariate Cox regression analyses

A survival package was used for Cox regression analysis, and forestplot package was adopted for drawing of a forest map to report the *P* value, HR, and 95% CI of every variable. According to the results of multivariate Cox proportional hazard analysis, the rms package was adopted to establish a nomogram to predict the 3- and 5-year survival rates. The nomogram provided a graphical representation of these factors, and the risk for an individual patient can be calculated by the points associated with every risk factor.

Baseline data

Totally 55 children with MB treated in Affiliated Ezhou Central Hospital (201611051) from January 2017 to January 2019 were enrolled into the patient group, and 30 healthy children who underwent physical examination in our hospital during the same period were assigned to the control group. The inclusion criteria: (1) Children confirmed with MB by head MRI; (2) Children ≤15 years old; (3) Children with expected survival ≥3 months; (4) Children and their families who were apprised of the study and provided signature on informed consent forms. The exclusion criteria: (1) Children with other tumors; (2) Children with congenital functional defects; (3) Children who were lost to follow up or failed to complete this treatment plan during the treatment process. This study was approved by the Medical Ethics Committee of Affiliated Ezhou Central Hospital (ethics approval number: 201611051). All patients were followed up for 3 years, and their survival was recorded.

Real time-quantitative polymerase chain reaction (RT-qPCR)

Total RNA was extracted from the collected serum of every patient and reverse-transcribed into cDNA with TaqMan small RNA Assays (Applied Biosystems™, USA, 4440418) and PrimeScript RT kits (Thermo Scientific™, USA, K1642). Then, the mRNA was treated by SYBR PreMix Ex Taq™II (TAKARA, Japan, RR820A), respectively, under a ABI PRISM7500 fast real-time qPCR system (Application Biossystems, Switzerland). The reaction system and reaction conditions were set according to instructions of the kits. $2^{-\Delta\Delta cT}$ was adopted for data analyses (internal reference for mRNA: GAPDH) [23]. The primer sequences are summarized in **Table 2**.

Statistical analyses

All figures and data of the bioinformatic analysis were completed by R (v4.0.3). GraphadPrism8.0 (La Jolla, California) was used to visualize the data. Measured data were expressed by mean ± standard deviation, and the independent sample t-test was used for comparison between groups. Counted data were expressed by % and analyzed by chi-square test. The K-M test was utilized to analyse the survival of children. $P<0.05$ denoted a significant difference.

Results

Synthesis of matrix files

Through the inSilicoMerging package, we acquired the before_merge.txt file via merging, and then acquired the matrix after_merge.txt with the batch effect eliminated by eliminating the batch effect. The box line diagram and density map (**Figure 1A**, **1B**) showed that the sample distribution of every data set was quite different before elimination of the batch effect, indicating the existence of a batch effect. In addition, the data distribution among every data set tended to be consistent after elimination of the batch effect. According to the Umap diagram (**Figure 1C**), the samples of every data set gathered together separately before elimination of the batch effect, indicating the existence of a batch effect, and the samples of each data set were clustered and interwoven

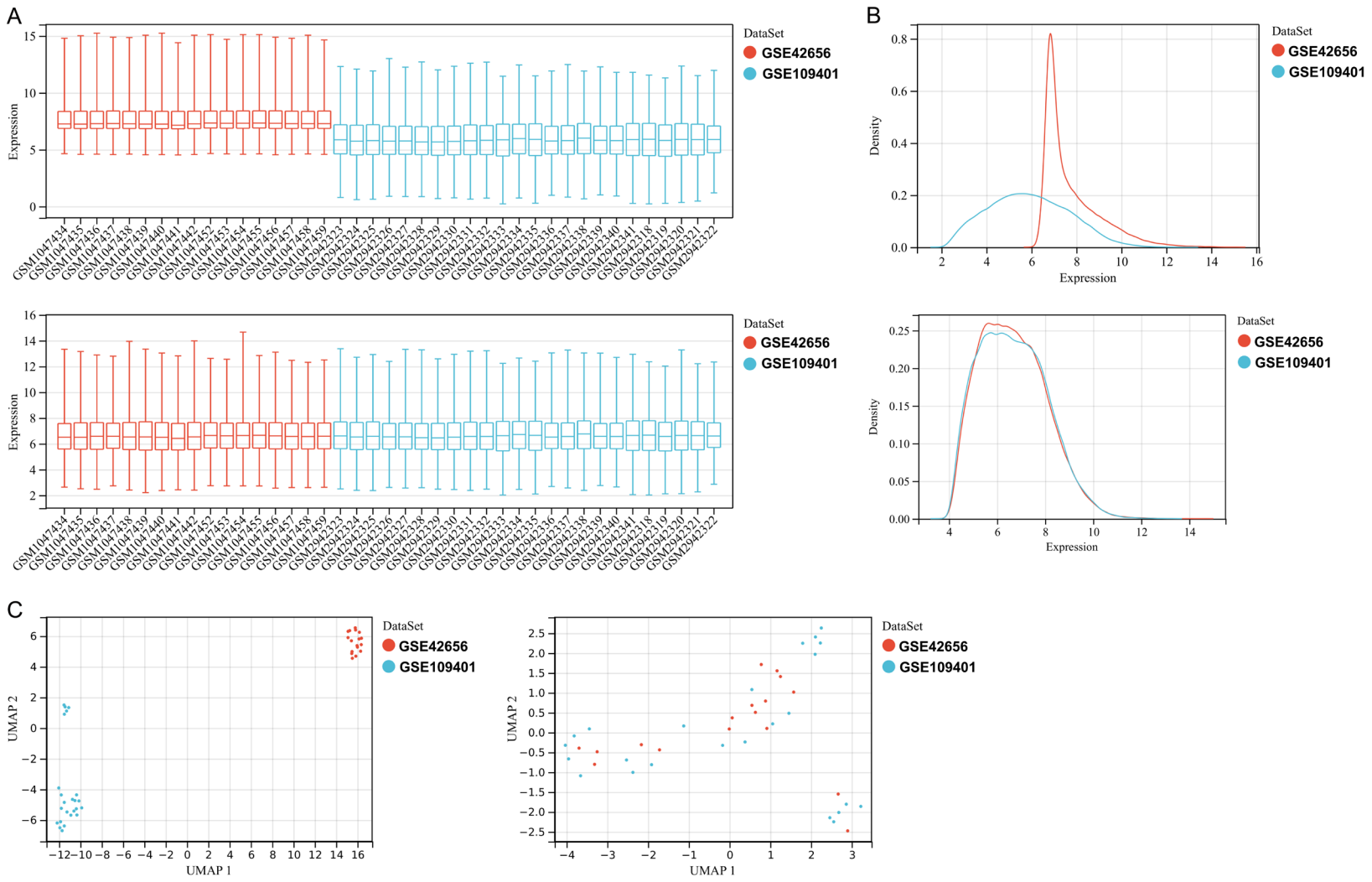

Figure 1. Matrix file with elimination of batch effect. A. Box line diagram before and after elimination of batch effect. B. Density map before and after elimination of batch effect. C. Umap diagram before and after elimination of batch effect.

with each other after elimination of it, indicating the successful elimination of the batch effect.

DEG identification and function analysis

The limma package was adopted to analyze the matrix file. With a threshold of Log FC: 2 and the FDR value <0.05, we found 247 DEGs in total, including 65 up-regulated ones and 182 down-regulated ones (**Figure 2A**, **2B**). Subsequently, 247 genes were functionally analyzed by clusterProfiler, GO and KEGG enrichment. In the GO enrichment, we found that DEGs were associated with 113 functions, which were strongly correlated with nervous system development, generation of neurons, neurogenesis, neuron differentiation, regulation of nervous system development, neuron parts, system development, synapse, cell development, and regulation of neurogenesis. According to KEGG analysis, DEG were involved in the process of 14 pathways, which were closely correlated to cell adhesion molecules, phospholipase D signaling pathway, Rap1 signaling pathway, cell cycle, oocyte meiosis, progesterone-mediated oocyte maturation, alanine, aspartate and glutamate metabolism, insulin secretion, Ras signaling pathway, and axon guidance (**Figure 3A**, **3B**).

Survival-associated Hub gene analysis

Thirty patients with a follow-up period of over 30 days from the GSE30074 data set were included in the survival analysis. Based on univariate Cox regression analysis, 9 key genes were found to be closely correlated with OS. Then, 6 genes (ASCL1, NLGN2, ASPA, C1orf61, AMPH and PTGDS) were identified by Lasso-Cox analysis to construct the prognostic model (**Figure 4A**, **4B**). The HR of every MB patient was calculated: HR=(0.7078)*ASCL1+(-5.664)*NLGN2+(-0.9477)*ASPA+(0.4787)*C1orf61+(-0.5131)*AMPH+(1.9627)*PTGDS. According to the median HR, MB patients were assigned to low- or high-risk groups (**Figure 4C**). K-M survival analysis revealed that the high-risk group showed a lower OS than the low-risk group (P<0.001, **Figure 4D**). Additionally, the sensitivity and specificity of this model in forecasting the OS of patients were verified by ROC curves, and the risk model showed good accuracy in forecasting the survival within 1, 2, and 3 years after operation (**Figure 4E**).

Univariate and multivariate Cox regression analyses of DEGs

This study was designed to analyse whether ASCL1, NLGN2, ASPA, C1orf61, AMPH, and PTGDS genes were independent prognostic factors of MB. According to univariate and multivariate Cox regression analyses, NLGN2 and PTGDS were probable independent prognostic factors of MB (**Figure 5A**, **5B**). For the purpose of developing a clinically applicable method for prediction of the survival probability of patients, we used a Nomogram chart to build the prediction model, and we generated the Nomogram chart to predict the OS in 1, 3 and 5 years by Cox regression (**Figure 5C**). As a result, compared to the ideal model in the whole queue, the calibration charts of OS in 1, 3, and 5 years were well predicted (**Figure 5D**).

Analysis of baseline data

The comparison of the clinical data between the two groups revealed no significant difference between them in age, gender, time of delivery of mother, or history of mother's abortion (P>0.05, **Table 3**).

Expression of NLGN2 and PTGDS in MB children

We collected the serum of MB children and quantified NLGN2 and PTGDS in it by RT-qPCR. The results revealed lower expression of NLGN2 and PTGDS in MB children than that of controls (P<0.001, **Figure 6**). In light of their median expression, patients were assigned to high- or low-expression groups, and their differences in clinical data were compared. The results revealed a higher proportion of tumour diameter ≥3 cm in the low expression group than that of the high expression group (P<0.05, **Table 4**).

Association of NLGN2 and PTGDS with patients' prognosis

All patients were followed up for three years, with a follow-up rate of 100%. In the light of NLGN2 and PTGDS expression, the patients were assigned to high- or low-expression groups, and the associations of NLGN2 and PTGDS with patients' survival were analysed. The results revealed a lower survival rate in the low NLGN2 and PTGDS expression groups than

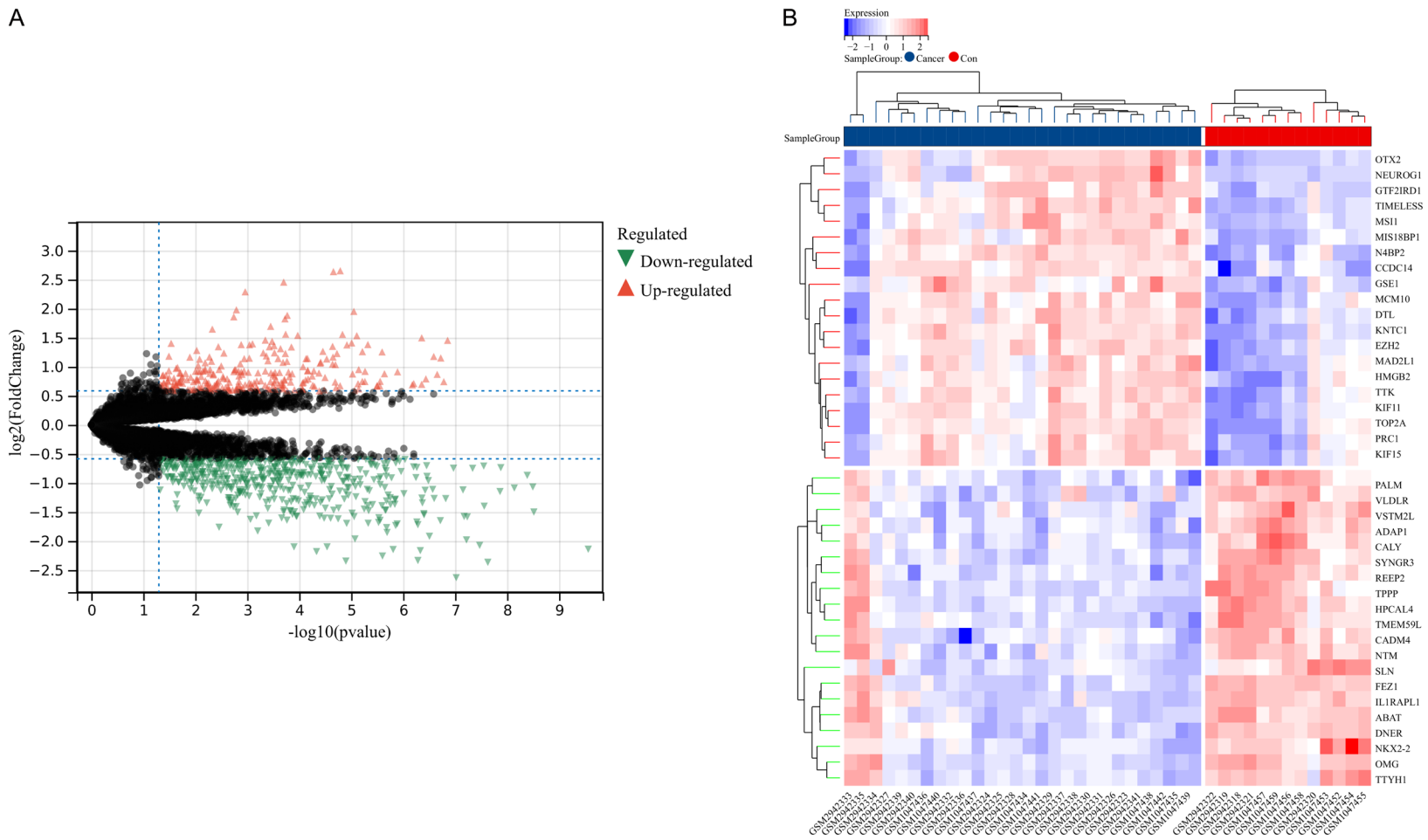

Figure 2. Matrix files for DEG analysis. A. Analysis of DEG volcano map in matrix files by Limma Package. B. Analysis of DEG heatmap in matrix files by heatmap.2 package. Note: Differentially expressed genes (DEGs).

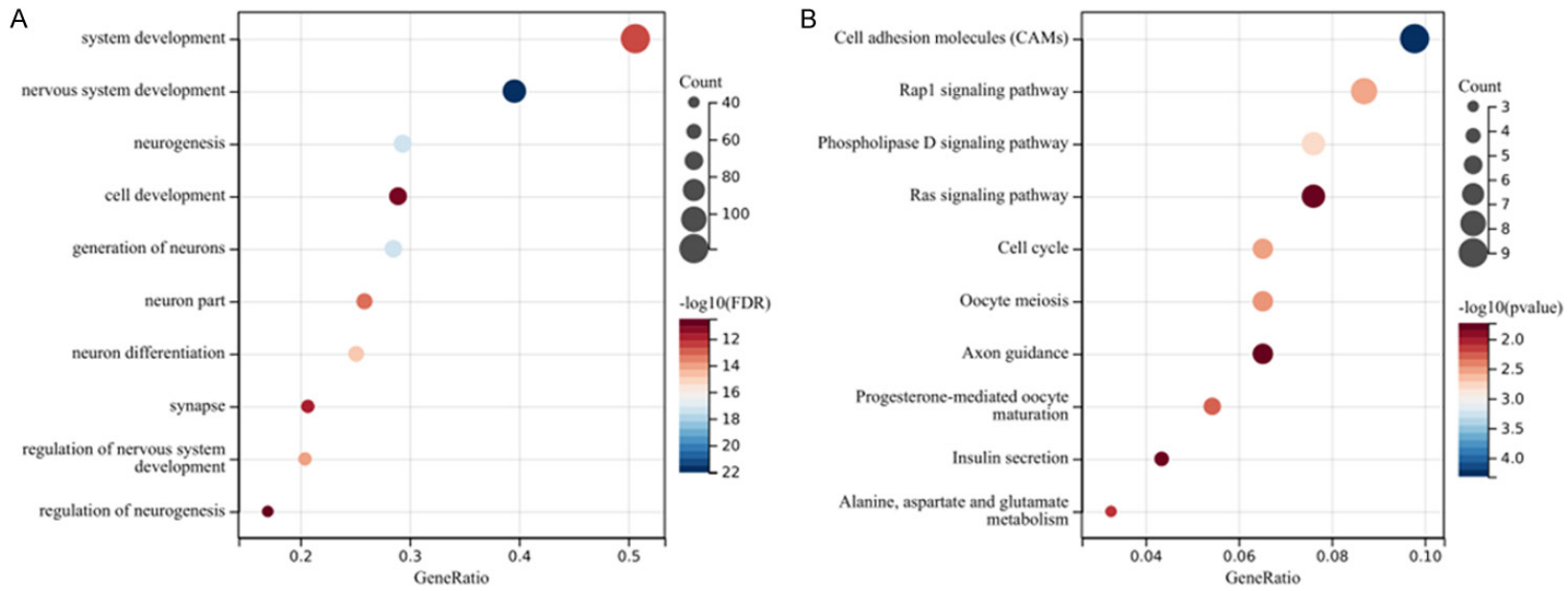

Figure 3. Function analysis of DEGs. A. Analysis of the functions implicated in DEGs (Top10) by GO enrichment. B. Analysis of the functions implicated in DEGs (Top10) by KEGG enrichment. Note: Gene Ontology (GO); Kyoto Encyclopedia of Genes and Genomes (KEGG); Differentially expressed genes (DEGs).

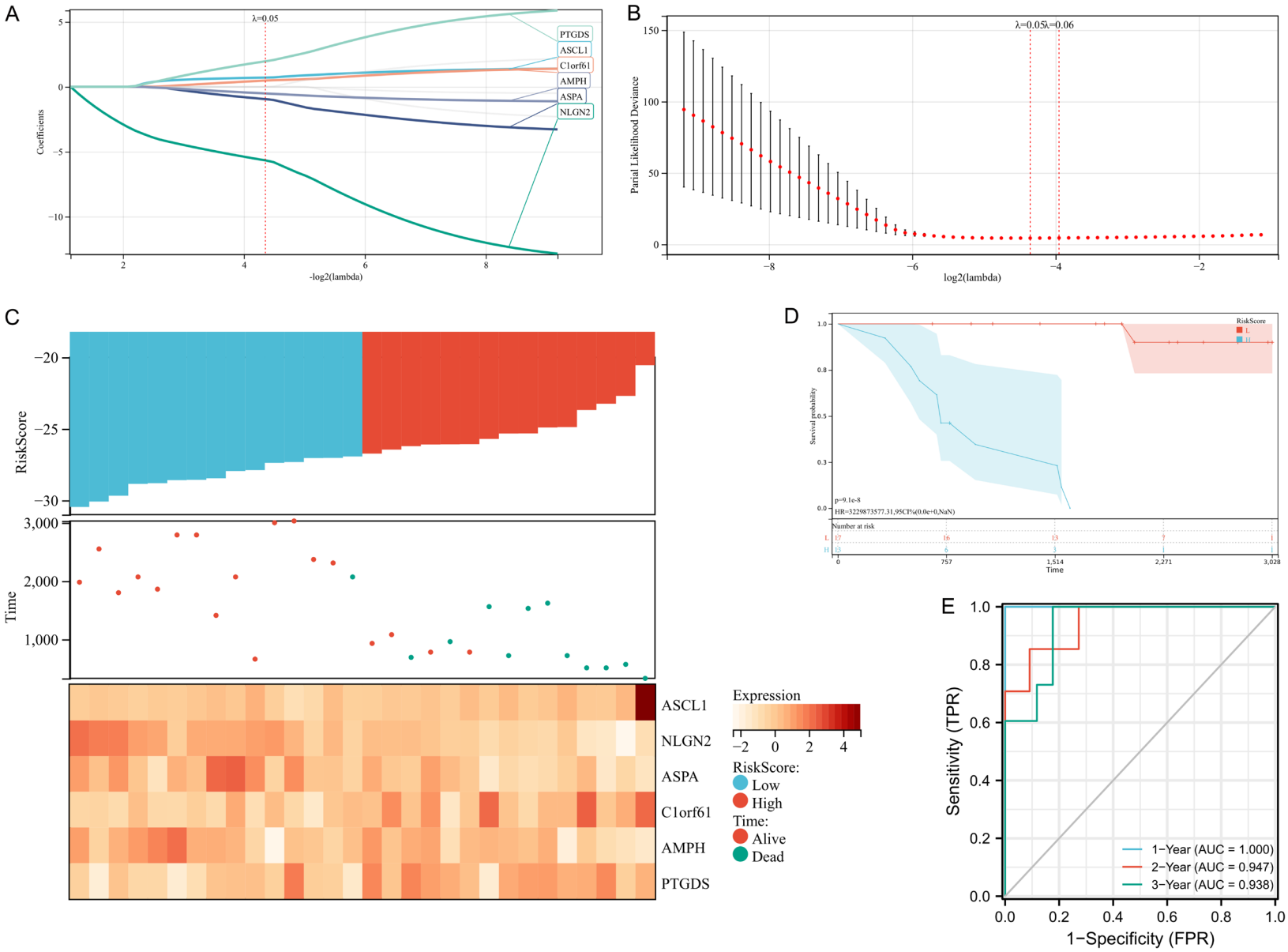

Figure 4. Survival model established by Lasso-Cox. A, B. The solution path of LASSO model and the association of the mean square error (CVMSE) of cross-validation with the size of the model. C. HR-based grouping of MB patients, and the expression of ASCL1, NLGN2, ASPA, C1orf61, AMPH, and PTGDS in the groups. D. K-M

curves of the high- and low-risk groups. E. Verification of prediction efficiency of the LASSO model for survival within 1, 2 and 3 years by time-dependent ROC curves. Note: Receiver operating characteristic (ROC); Hazard risk (HR); Kaplan-Meier (K-M); Achaete-scute family bHLH transcription factor 1 (ASCL1); Neuroligin 2 (NLGN2); Aspartoacylase (ASPA); Amphiphysin (AMPH); Prostaglandin D2 synthase (PTGDS); Medulloblastoma (MB).

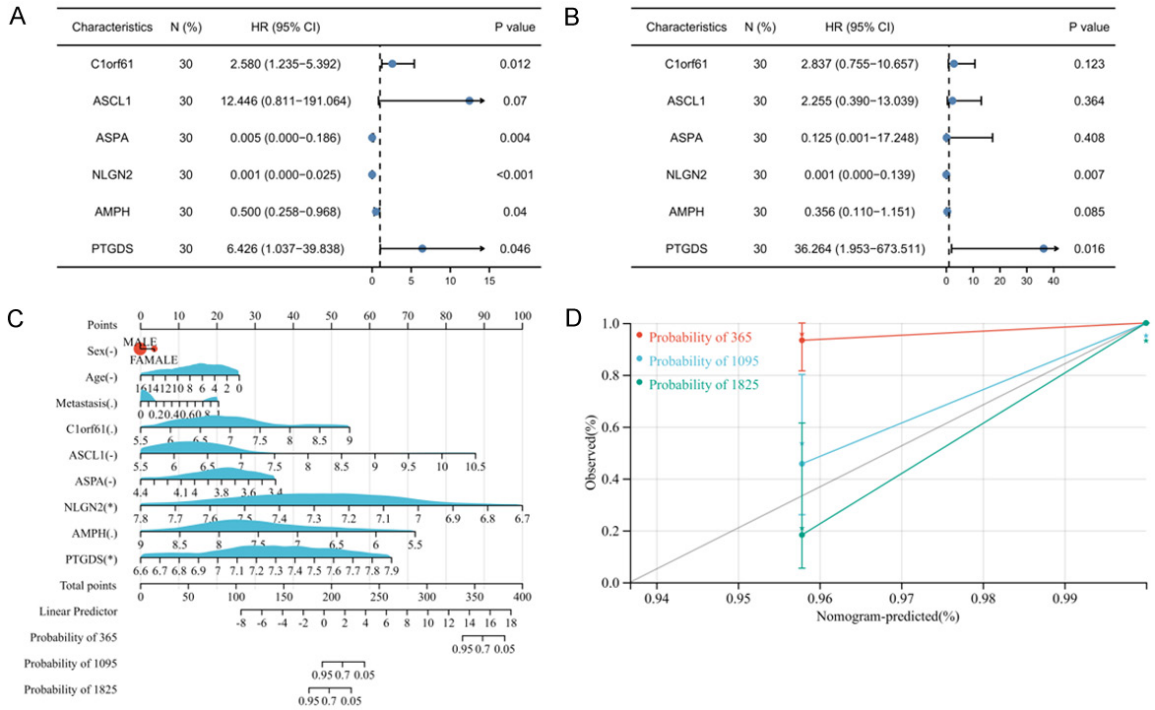

Figure 5. Construction of Nomogram chart. A, B. Univariate and multivariate Cox analysis of *P* value, HR, and confidence interval of the expression and clinical features of DEGs. C. Nomogram can forecast the 1-, 3- and 5-year OS of patients with MB. D. The calibration curve of the nomogram model of OS in the group. Note: Hazard risk (HR); Kaplan-Meier (K-M); Medulloblastoma (MB); Overall survival (OS); Differentially expressed genes (DEGs).

in the other corresponding groups (P<0.05, **Figure 7**).

Discussion

Medulloblastoma (MB) is one of the most common malignant central nervous system and brain tumors in children, and it has been classified as a high-risk disease because of its unsatisfactory prognosis [24]. With the development of molecular subgroups, genetic testing plays an important role in the classification and treatment of MB [25]. Studies have revealed that most SHH-MB patients have genetic mutations and copy number changes of key genes in the SHH signaling pathway, and some mutations and changes were associated with poor patient prognosis [26-29]. For example, earlier studies found that 22 subtype-specific gene signatures could help predict molecular subpopulations in 88% of recent formalin-fixed paraffin-embedded (FFPE) medulloblastoma samples [30]. Another study found that a total of 82 differential microRNAs were deleted from 30 medulloblastoma cases by analyzing the GEO dataset, and miR-135a and miR-146b were found to be related to the occurrence of medulloblastoma [31].

In the present study, we integrated the GSE-109401 and GSE42656 datasets to obtain DEGs between MB tissue and normal brain tissue. Then we selected 247 DEGs and found, using enrichment analysis, that DEGs were associated with nervous system development, neuronal phylogeny, neuronal differentiation, neuronal parts, phylogeny, regulation of neurogenesis, regulation of neurogenesis development, and discovery of cell-related regulation. This suggested that the DEGs we obtained were closely related to brain function, and further survival analysis revealed 9 hub genes

Table 3. Comparison of baseline data [n (%)]

Factor	Patient group (n=55)	Control group (n=30)	*P* value
Age			0.222
≥3 years old	35 (63.64)	15 (50.00)	
<3 years old	20 (36.36)	15 (50.00)	
Gender			0.765
Male	22 (40.00)	13 (43.33)	
Female	33 (60.00)	17 (56.67)	
Times of delivery of mother			0.502
Primipara	18 (32.73)	12 (40.00)	
Multipara	37 (67.27)	18 (60.00)	
Abortion history of mother			0.558
Yes	15 (27.27)	10 (33.33)	
No	40 (72.73)	20 (66.67)	
Tumor diameter			
≥3 cm	14 (25.46)		
<3 cm	41 (74.55)		
Tumor site			
Vermis cerebelli	23 (41.82)		
Cerebellar hemispheres	32 (58.18)		
Histologic classification			
Classic	37 (67.27)		
Other	18 (32.73)		
Molecular subtype			
WNT	13 (23.63)		
SHH	12 (21.82)		
Non WNT/SHH	30 (54.55)		

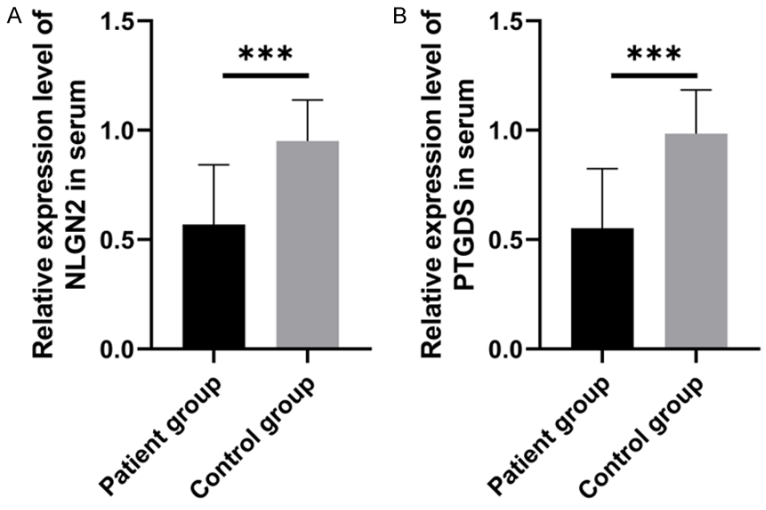

Figure 6. Serum NLGN2 and PTGDS in MB patients and healthy children. A. Quantification of serum NLGN2 in MB patients by RT-qPCR. B. Quantification of serum PTGDS in MB patients by RT-qPCR. Note: ***P<0.001; Neuroligin 2 (NLGN2); Prostaglandin D2 synthase (PTGDS); Real time-quantitative polymerase chain reaction (RT-qPCR); Medulloblastoma (MB).

associated with overall survival. LASSO and multivariate Cox analysis further narrowed the range of markers and established risk models for predicting MB prognosis. Moreover, six gene signatures for predicting the overall survival of MB patients were established by Lasso Cox regression. Low expression of ASCL1, NLGN2, ASPA, C1orf-61, AMPH, and PTGDS were identified as protective genes and correlated with poor survival. We evaluated model performance using ROC curves for twelve-gene signatures, which showed that the area under the ROC curve of the 1-year, 2-year and 3-year survival prediction models was greater than 0.9, indicating that the gene signature has high sensitivity and specificity. Finally, by establishing a prognostic model, we derived a prognostic gene marker panel (NLGN2, PTGDS) that divides the OS of MB patients into low-risk and high-risk subgroups, and Cox regression analysis showed that the NLGN2 and PTGDS panel could be used as independent prognostic markers. In the study of Yang et al. [32], a total of 1006 common differential genes were screened through 4 GEO chips, and the underlying mechanism of MB was analyzed by enrichment analysis and construction of a protein-protein interaction network. However, we constructed an MB prognosis model through Lasso in the present study, which better predicted the prognosis of patients through risk scores.

NLGN2 is a member of the neuronal cell surface protein

Table 4. Analysis of NLGN2, PTGDS, and clinical data

Factor	NLGN2		*P* value	PTGDS		*P* value
	High expression (n=27)	Low expression (n=28)		High expression (n=27)	Low expression (n=28)	
Age			0.221			0.919
≥3 years old (n=35)	15 (55.56)	20 (71.43)		17 (62.96)	18 (64.29)	
<3 years old (n=20)	12 (44.44)	8 (28.57)		10 (37.04)	10 (35.71)	
Gender			0.509			0.660
Male (n=22)	12 (44.44)	10 (35.71)		10 (37.04)	12 (42.86)	
Female (n=33)	15 (55.56)	18 (64.29)		17 (62.96)	16 (57)	
Tumor diameter			0.017			0.003
≥3 cm (n=14)	3 (11.11)	11 (39.29)		2 (7.41)	12 (42.86)	
<3 cm (n=41)	24 (88.89)	17 (60.71)		25 (92.59)	16 (57.14)	
Tumor site			0.210			0.350
Vermis cerebelli (n=23)	9 (33.33)	14 (50.00)		13 (48.15)	10 (35.71)	
Cerebellar hemisphere (n=32)	18 (66.67)	14 (50.00)		14 (51.85)	18 (64.29)	
Histologic classification			0.504			0.291
Classic (n=37)	17 (62.96)	20 (71.43)		20 (74.07)	17 (60.71)	
Other (n=18)	10 (37.04)	8 (28.57)		7 (25.93)	11 (39.29)	
Molecular subtype			0.728			0.198
WNT (n=13)	8 (29.63)	6 (21.43)		7 (25.93)	5 (17.86)	
SHH (n=12)	5 (18.52)	7 (25.00)		8 (29.63)	4 (14.28)	
Non WNT/SHH (n=30)	14 (51.85)	15 (51.72)		12 (44.44)	19 (67.86)	

Note: Neuroligin 2 (NLGN2); Prostaglandin D2 synthase (PTGDS).

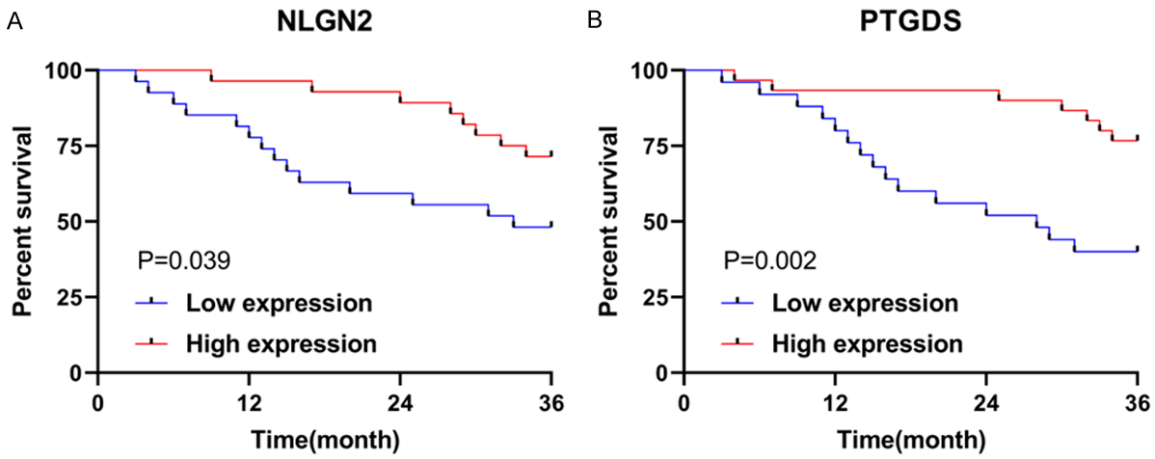

Figure 7. Analysis of the associations of NLGN2 and PTGDS with the survival of patients. A. Analysis of the association of NLGN2 with 3-year survival of MB patients by K-M survival curve. B. Analysis of the association of PTGDS with 3-year survival of MB patients by K-M survival curve. Note: Neuroligin 2 (NLGN2); Prostaglandin D2 synthase (PTGDS); Medulloblastoma (MB); Kaplan-Meier (K-M).

family that can act as splice site-specific ligands for β-neurexins individually and may be involved in CNS synapse formation and remodelling [33]. In the study of Katzman et al. [34], it was found that changes in NLGN2 expression regulated the dynamic process of memory consolidation and reinforcement. PTGDS is a glutathione-independent prostaglandin D synthase with the ability to catalyze the conversion of prostaglandin H2 (PGH2) to prostaglandin D2 (PGD2) [35]. Studies have shown that PTGDS was preferentially expressed in the brain and

its overexpression was involved in the regulation of non-REM sleep [36]. In the present study, we reported the value of NLGN2 and PTGDS in MB for the first time through bioinformatic analysis. In addition, we found through clinical sample analysis that NLGN2 and PTGDS presented low expression in the serum of MB children, and follow-up visit suggested that the 3-year survival rate of patients with low NLGN2 and PTGDS expression was significantly reduced. This is the first time we have found the clinical value of NLGN2 and PTGDS in MB, suggesting that NLGN2 and PTGDS may be predictors of MB. However, this study still has some limitations. First, the limited sample size of the prognostic data set and large span between patient survivals may lead to bias in the data analysis. Second, we failed to validate the dataset with external data. Finally, the follow-up time of this study is short, and we need to further verify whether NLGN2 and PTGDS have value in the long-term prognosis of patients. Therefore, we hope to expand the sample size collection in future studies to validate our results through more clinical experiments.

In conclusion, our results systematically demonstrated the expression, potential function, and prognostic value of NLGN2, and PTGDS in MB, which provides a new basis for tumor gene-targeted therapy and prognosis.

Disclosure of conflict of interest

None.

Address correspondence to: Wei Jiang, Department of Neurosurgery, Tongji Hospital, Tongji Medical College, Huazhong University of Science & Technology, 1095# Jiefang Avenue, Wuhan 430030, Hubei, PR China. Tel: +86-027-83665200; E-mail: dr.jiangwei@tjh.tjmu.edu.cn

References

[1] Millard NE and De Braganca KC. Medulloblastoma. J Child Neurol 2016; 31: 1341-1353.

[2] Menyhart O and Gyorffy B. Molecular stratifications, biomarker candidates and new therapeutic options in current medulloblastoma treatment approaches. Cancer Metastasis Rev 2020; 39: 211-233.

[3] Bray F, Ferlay J, Soerjomataram I, Siegel RL, Torre LA and Jemal A. Global cancer statistics 2018: GLOBOCAN estimates of incidence and mortality worldwide for 36 cancers in 185 countries. CA Cancer J Clin 2018; 68: 394-424.

[4] Northcott PA, Robinson GW, Kratz CP, Mabbott DJ, Pomeroy SL, Clifford SC, Rutkowski S, Ellison DW, Malkin D, Taylor MD, Gajjar A and Pfister SM. Medulloblastoma. Nat Rev Dis Primers 2019; 5: 11.

[5] Franchino F, Morra I, Forni M, Bertero L, Zanini C, Roveta F, Ricardi U, Mantovani C, Carpaneto A, Migliore E, Pellerino A, Ferrio F, Cassoni P, Garbossa D, Soffietti R and Ruda R. Medulloblastoma in adults: an analysis of clinico-pathological, molecular and treatment factors. J Neurosurg Sci 2021; [Epub ahead of print].

[6] Liu X, Ding C, Tan W and Zhang A. Medulloblastoma: molecular understanding, treatment evolution, and new developments. Pharmacol Ther 2020; 210: 107516.

[7] Quinlan A and Rizzolo D. Understanding medulloblastoma. JAAPA 2017; 30: 30-36.

[8] Samkari A, White J and Packer R. SHH inhibitors for the treatment of medulloblastoma. Expert Rev Neurother 2015; 15: 763-770.

[9] Caimano M, Lospinoso Severini L, Loricchio E, Infante P and Di Marcotullio L. Drug delivery systems for hedgehog inhibitors in the treatment of SHH-medulloblastoma. Front Chem 2021; 9: 688108.

[10] Yu J and Li H. The expression of FAT1 is associated with overall survival in children with medulloblastoma. Tumori 2017; 103: 44-52.

[11] Cook Sangar ML, Genovesi LA, Nakamoto MW, Davis MJ, Knobluagh SE, Ji P, Millar A, Wainwright BJ and Olson JM. Inhibition of CDK4/6 by palbociclib significantly extends survival in medulloblastoma patient-derived xenograft mouse models. Clin Cancer Res 2017; 23: 5802-5813.

[12] Clough E and Barrett T. The gene expression omnibus database. Methods Mol Biol 2016; 1418: 93-110.

[13] Rivero-Hinojosa S, Lau LS, Stampar M, Staal J, Zhang H, Gordish-Dressman H, Northcott PA, Pfister SM, Taylor MD, Brown KJ and Rood BR. Proteomic analysis of Medulloblastoma reveals functional biology with translational potential. Acta Neuropathol Commun 2018; 6: 48.

[14] Henriquez NV, Forshew T, Tatevossian R, Ellis M, Richard-Loendt A, Rogers H, Jacques TS, Reitboeck PG, Pearce K, Sheer D, Grundy RG and Brandner S. Comparative expression analysis reveals lineage relationships between human and murine gliomas and a dominance of glial signatures during tumor propagation in vitro. Cancer Res 2013; 73: 5834-5844.

[15] Park AK, Lee SJ, Phi JH, Wang KC, Kim DG, Cho BK, Haberler C, Fattet S, Dufour C, Puget S, Sainte-Rose C, Bourdeaut F, Grill J, Delattre O, Kim SK and Park WY. Prognostic classification of pediatric medulloblastoma based on chromosome 17p loss, expression of MYCC and MYCN, and Wnt pathway activation. Neuro Oncol 2012; 14: 203-214.

[16] Taminau J, Meganck S, Lazar C, Steenhoff D, Coletta A, Molter C, Duque R, de Schaetzen V, Weiss Solis DY, Bersini H and Nowe A. Unlocking the potential of publicly available microarray data using inSilicoDb and inSilicoMerging R/Bioconductor packages. BMC Bioinformatics 2012; 13: 335.

[17] Johnson WE, Li C and Rabinovic A. Adjusting batch effects in microarray expression data using empirical bayes methods. Biostatistics 2007; 8: 118-127.

[18] Ritchie ME, Phipson B, Wu D, Hu Y, Law CW, Shi W and Smyth GK. Limma powers differential expression analyses for RNA-sequencing and microarray studies. Nucleic Acids Res 2015; 43: e47.

[19] Yu G, Wang LG, Han Y and He QY. clusterProfiler: an R package for comparing biological themes among gene clusters. OMICS 2012; 16: 284-287.

[20] Gene Ontology Consortium. Gene ontology consortium: going forward. Nucleic Acids Res 2015; 43: D1049-1056.

[21] Kanehisa M and Goto S. KEGG: kyoto encyclopedia of genes and genomes. Nucleic Acids Res 2000; 28: 27-30.

[22] Yang L, Qu Q, Hao Z, Sha K, Li Z and Li S. Powerful identification of large quantitative trait loci using genome-wide R/glmnet-based regression. J Hered 2022; [Epub ahead of print].

[23] Livak KJ and Schmittgen TD. Analysis of relative gene expression data using real-time quantitative PCR and the 2(-delta delta C(T)) method. Methods 2001; 25: 402-408.

[24] Kanemura Y. Medulloblastoma. No Shinkei Geka 2022; 50: 73-90.

[25] Cotter JA and Hawkins C. Medulloblastoma: WHO 2021 and beyond. Pediatr Dev Pathol 2022; 25: 23-33.

[26] Ghasemi DR, Fleischhack G, Milde T and Pajtler KW. The current landscape of targeted clinical trials in non-WNT/non-SHH medulloblastoma. Cancers (Basel) 2022; 14: 679.

[27] Ramaswamy V, Remke M, Bouffet E, Bailey S, Clifford SC, Doz F, Kool M, Dufour C, Vassal G, Milde T, Witt O, von Hoff K, Pietsch T, Northcott PA, Gajjar A, Robinson GW, Padovani L, Andre N, Massimino M, Pizer B, Packer R, Rutkowski S, Pfister SM, Taylor MD and Pomeroy SL. Risk stratification of childhood medulloblastoma in the molecular era: the current consensus. Acta Neuropathol 2016; 131: 821-831.

[28] Waszak SM, Northcott PA, Buchhalter I, Robinson GW, Sutter C, Groebner S, Grund KB, Brugières L, Jones DTW, Pajtler KW, Morrissy AS, Kool M, Sturm D, Chavez L, Ernst A, Brabetz S, Hain M, Zichner T, Segura-Wang M, Weischenfeldt J, Rausch T, Mardin BR, Zhou X, Baciu C, Lawerenz C, Chan JA, Varlet P, Guerrini-Rousseau L, Fults DW, Grajkowska W, Hauser P, Jabado N, Ra YS, Zitterbart K, Shringarpure SS, De La Vega FM, Bustamante CD, Ng HK, Perry A, MacDonald TJ, Hernáiz Driever P, Bendel AE, Bowers DC, McCowage G, Chintagumpala MM, Cohn R, Hassall T, Fleischhack G, Eggen T, Wesenberg F, Feychting M, Lannering B, Schüz J, Johansen C, Andersen TV, Röösli M, Kuehni CE, Grotzer M, Kjaerheim K, Monoranu CM, Archer TC, Duke E, Pomeroy SL, Shelagh R, Frank S, Sumerauer D, Scheurlen W, Ryzhova MV, Milde T, Kratz CP, Samuel D, Zhang J, Solomon DA, Marra M, Eils R, Bartram CR, von Hoff K, Rutkowski S, Ramaswamy V, Gilbertson RJ, Korshunov A, Taylor MD, Lichter P, Malkin D, Gajjar A, Korbel JO and Pfister SM. Spectrum and prevalence of genetic predisposition in medulloblastoma: a retrospective genetic study and prospective validation in a clinical trial cohort. Lancet Oncol 2018; 19: 785-798.

[29] Reis J, Stahl R, Zimmermann H, Ruf V, Thon N, Kunz M, Liebig T and Forbrig R. Advanced MRI findings in medulloblastomas: relationship to genetic subtypes, histopathology, and immunohistochemistry. J Neuroimaging 2021; 31: 306-316.

[30] Northcott PA, Shih DJ, Remke M, Cho YJ, Kool M, Hawkins C, Eberhart CG, Dubuc A, Guettouche T, Cardentey Y, Bouffet E, Pomeroy SL, Marra M, Malkin D, Rutka JT, Korshunov A, Pfister S and Taylor MD. Rapid, reliable, and reproducible molecular sub-grouping of clinical medulloblastoma samples. Acta Neuropathol 2012; 123: 615-626.

[31] Tantawy M, Elzayat MG, Yehia D and Taha H. Identification of microRNA signature in different pediatric brain tumors. Genet Mol Biol 2018; 41: 27-34.

[32] Yang B, Dai JX, Pan YB, Ma YB, Chu SH. Examining the biomarkers and molecular mechanisms of medulloblastoma based on bioinformatics analysis. Oncol Lett 2019; 18: 433-441.

[33] Kathuria A, Lopez-Lengowski K, Watmuff B, McPhie D, Cohen BM and Karmacharya R. Synaptic deficits in iPSC-derived cortical interneurons in schizophrenia are mediated by NLGN2 and rescued by N-acetylcysteine. Transl Psychiatry 2019; 9: 321.

[34] Katzman A and Alberini CM. NLGN1 and NLGN2 in the prefrontal cortex: their role in memory consolidation and strengthening. Curr Opin Neurobiol 2018; 48: 122-130.
[35] Hu S, Ren S, Cai Y, Liu J, Han Y, Zhao Y, Yang J, Zhou X and Wang X. Glycoprotein PTGDS promotes tumorigenesis of diffuse large B-cell lymphoma by MYH9-mediated regulation of Wnt-beta-catenin-STAT3 signaling. Cell Death Differ 2022; 29: 642-656.
[36] Ding M and Toth LA. mRNA expression in mouse hypothalamus and basal forebrain during influenza infection: a novel model for sleep regulation. Physiol Genomics 2006; 24: 225-234.